Letter

Percolation theory of self-exciting temporal processes

Daniele Notarmuzi,[1] Claudio Castellano,[2] Alessandro Flammini,[1] Dario Mazzilli,[1] and Filippo Radicchi[1,*]

[1]*Center for Complex Networks and Systems Research, Luddy School of Informatics, Computing, and Engineering, Indiana University, Bloomington, Indiana 47408, USA*

[2]*Istituto dei Sistemi Complessi (ISC-CNR), Via dei Taurini 19, I-00185 Rome, Italy*

(Received 19 August 2020; accepted 5 February 2021; published 24 February 2021)

We investigate how the properties of inhomogeneous patterns of activity, appearing in many natural and social phenomena, depend on the temporal resolution used to define individual bursts of activity. To this end, we consider time series of microscopic events produced by a self-exciting Hawkes process, and leverage a percolation framework to study the formation of macroscopic bursts of activity as a function of the resolution parameter. We find that the very same process may result in different distributions of avalanche size and duration, which are understood in terms of the competition between the 1D percolation and the branching process universality class. Pure regimes for the individual classes are observed at specific values of the resolution parameter corresponding to the critical points of the percolation diagram. A regime of crossover characterized by a mixture of the two universal behaviors is observed in a wide region of the diagram. The hybrid scaling appears to be a likely outcome for an analysis of the time series based on a reasonably chosen, but not precisely adjusted, value of the resolution parameter.

DOI: 10.1103/PhysRevE.103.L020302

Inhomogeneous patterns of activity, characterized by bursts of events separated by periods of quiescence, are ubiquitous in nature [1]. The firing of neurons [2,3], earthquakes [4], energy release in astrophysical systems [5], and spreading of information in social systems [6–8] exhibit bursty activity, with intensity and duration of bursts obeying power-law distributions [2,3,7].

If activity consists of pointlike events in time, size and duration of bursts are obtained from the interevent time sequence. The analysis of many systems [4,6,7,9,10] reveals that the interevent time between consecutive events has a fat-tailed distribution [4,6,7]. This distribution appears more reliable for the characterization of correlation in bursty systems than other traditional measures, e.g., the autocorrelation function [7,11,12]. However, the relation between autocorrelation and burst size distribution is opaque. Further complications arise as the separation between different bursts is not clear-cut. In discrete time series, avalanches of correlated activity are monitored by coarsening the time series at a fixed temporal scale, and correlations are measured by assigning events to the same burst if their interevent time is smaller than a given threshold [7]. The threshold is set equal to some arbitrarily chosen value and/or imposed by the temporal resolution at which empirical data are acquired, despite its potential of affecting the properties of the resulting distributions [13–19].

The purpose of the present letter is to understand the relation between temporal resolution and burst statistics. We introduce a principled technique to determine the value of the time resolution that should be used to define avalanches from time series. We validate the method on time series generated according to an Hawkes process [20], a model of autocorrelated behavior used for the description of earthquakes [21,22], neuronal networks [23], and socioeconomic systems [24,25]. The use of the Hawkes process affords us a complete control over the mechanism that generates correlations and the possibility to attack the problem analytically.

We start by defining a cluster of activity consistently with the informal notion of a burst composed of close-by events. Data are represented by K total events $\{t_1, \ldots, t_K\}$, where t_i is the time of appearance of the ith event. We fix a resolution parameter $\Delta \geqslant 0$ to identify clusters of activity. A cluster starting at time t_b is given by the S consecutive events $\{t_b, t_{b+1}, \ldots, t_{b+S-1}\}$ such that $t_b - t_{b-1} > \Delta$, $t_{b+S} - t_{b+S-1} > \Delta$, and $t_{b+i} - t_{b+i-1} \leqslant \Delta$ for all $i = 1, \ldots, S$. We assume $t_0 = -\infty$ and $t_{K+1} = +\infty$, implying that the first and the last events open and close a cluster, respectively. We define the size S as the number of events within the cluster, and its duration as $T = t_{b+S-1} - t_b$, i.e., the time lag between the first and last event in the cluster.

If Δ is larger than the largest interevent time, then we have a single cluster of size K and duration $t_K - t_1$. On the other hand, if Δ is smaller than the smallest interevent time, each event is a cluster of size 1 and duration 0. As in 1D percolation problems [26], we expect for an intermediate value $\Delta = \Delta^*$ a transition from the nonpercolating to the percolating phase. What can we learn from the percolation diagram of the time series? Does fixing $\Delta = \Delta^*$ allow us to observe properties of the process otherwise not apparent?

We address the above questions in a controlled setting where we generate time series via an Hawkes process [20,27] with conditional rate

$$\lambda(t|t_1, \ldots, t_k) = \mu + n \sum_{i=1}^{k} \phi(t - t_i). \tag{1}$$

*Corresponding author: filiradi@indiana.edu

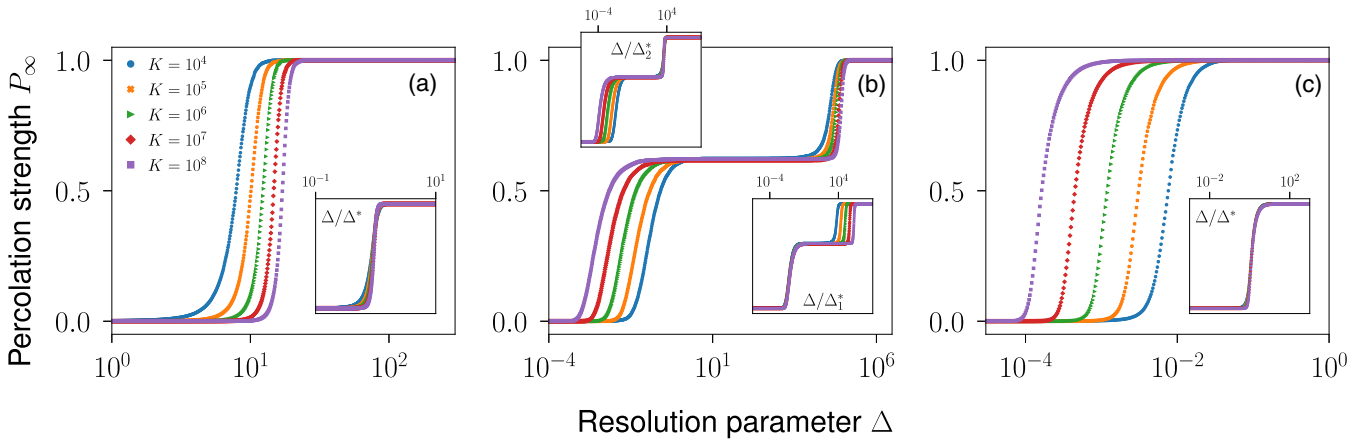

FIG. 1. Percolation phase diagrams of self-exciting temporal processes. We plot the percolation strength P_∞ as a function of the resolution parameter Δ for various configurations of the rate of Eq. (1), with exponential kernel function and various system sizes K. Average values are obtained by considering $R = 10^3$ realizations of the process. (a) We set $n = 0$ and $\mu = 1$. The inset shows the same data as of the main panel with abscissa rescaled as Δ/Δ^*. (b) We set $n = 1$ and $\mu = 10^{-4}$. The insets display the same data as of the main panel, but with rescaled abscissa, Δ/Δ_1^* in the lower inset, and Δ/Δ_2^* in the upper inset. (c) We set $n = 1$ and $\mu = 10^2$. The inset shows the same data as of the main panel, but with abscissa rescaled as Δ/Δ^*.

The rate depends on the k earlier events happened at times $t_1 \leqslant t_2 \leqslant \cdots \leqslant t_k \leqslant t$. The first term in Eq. (1) produces spontaneous events at rate $\mu \geqslant 0$. The second term consists of the sum of individual contributions from each earlier event, with the ith event happened at time $t_i \leqslant t$ increasing the rate by $\phi(t - t_i)$. $\phi(x)$ is the excitation or kernel function of the self-exciting process, and it is assumed to be non-negative and monotonically nonincreasing. Typical choices for the kernel are exponential or power-law decaying functions. We will consider both cases. In Eq. (1), we assume $\int_0^\infty \phi(x)\, dx = 1$, so that the memory term is weighted by the single parameter $n \geqslant 0$. Unless otherwise stated, we always set $n = 1$, corresponding to the critical dynamical regime of the temporal point process described by Eq. (1) [21].

The percolation framework allows us to characterize the generic Hawkes process of Eq. (1) using finite-size scaling analysis [26] (see Ref. [28], Sec. C). The total number K of events in the time series is the system size. For a given value of K, we generate multiple time series and compute the percolation strength P_∞, i.e., the fraction of events belonging to the largest cluster, and the associated susceptibility (see Ref. [28], Sec. C). By studying the behavior of these macroscopic observables as K grows, we estimate the values of the thresholds and the critical exponents.

Let us start with the case $n = 0$ [Fig. 1(a)], describing a homogeneous Poisson process with rate μ. The generic interevent time $x_i = t_i - t_{i-1}$ is a random variate distributed as $P(x_i) = \mu\, e^{-\mu x_i}$. Two consecutive events are part of the same cluster with probability $P(x_i \leqslant \Delta) = 1 - e^{-\mu\Delta}$, which is independent of the index i and represents an effective bond occupation probability in a homogeneous 1D percolation model [26,34]. For finite K values, P_∞ sharply grows from 0 to 1 around the pseudocritical point $\Delta^*(K) = \log(K)/\mu$ (see Ref. [28], Sec. D). Finite-size scaling analysis indicates that the transition is discontinuous, as expected for 1D ordinary percolation [26]. We note that the distributions of cluster size $P(S)$ and duration $P(T)$ are exactly described by the 1D percolation theory [26] (see Ref. [28], Sec. D). They are the product of a power-law function and a fast-decaying scaling function accounting for the system finite size [34]. In this specific case, the scaling functions contain a multiplicative term that exactly cancels the power-law term of the distribution. Therefore, the distributions have exponential behavior at $\Delta = \Delta^*$. A clear signature of criticality is manifest in the relation between size and duration, $\langle S\rangle \sim T$, in agreement with the relation $\langle S\rangle \sim T^{(\alpha-1)/(\tau-1)}$ (see Ref. [28], Sec. D).

We now consider the Hawkes process of Eq. (1) with exponential kernel $\phi(x) = e^{-x}$ [27,35]. Results of our finite-size scaling analysis are reported in Figs. 1(b) and 1(c), for $\mu \ll 1$ and $\mu \gg 1$, respectively.

For $\mu \ll 1$, the phenomenology is rich, with two distinct transitions at $\Delta_1^* < \Delta_2^*$, respectively. Around the critical point Δ_1^*, the system is characterized by a behavior compatible with the universality class of 1D percolation, i.e., the same as of the homogeneous Poisson process. Both $P(S)$ and $P(T)$ display power-law decays at Δ_1^*, with exponent values $\tau = \alpha = 2$ [Figs. 2(a) and 2(c)]. Average size and duration of clusters are linearly correlated (Ref. [28], Sec. E). The pseudocritical threshold equals $\Delta_1^*(K) \simeq \log(K)/\langle\lambda\rangle = \log(K)/(\mu + \sqrt{2K\mu})$, thus leading to a vanishing critical point in the thermodynamic limit (see Ref. [28], Sec. E). $\langle\lambda\rangle$ is the expectation value, over an infinite number of realizations of the process, of the rate after K events have happened; the estimate of the critical point $\Delta_1^*(K)$ is thus obtained using the same exact equation as for a homogeneous Poisson process with effective rate $\langle\lambda\rangle$. The other transition at $\Delta_2^*(K) = \log(K)/\mu$, which tends to infinite as K grows, corresponds to the merger of the whole time series into one cluster; its features are compatible with those of the universality class of the mean-field branching process, i.e., $\tau = 3/2$ and $\alpha = 2$. The region of the phase diagram $[\Delta_1^*(K), \Delta_2^*(K)]$, which is expanding as K increases, is characterized by critical behavior. While the percolation strength plateaus at $P_\infty \simeq 1 - 1/e \simeq 0.63$, the susceptibility is larger than zero. Furthermore,

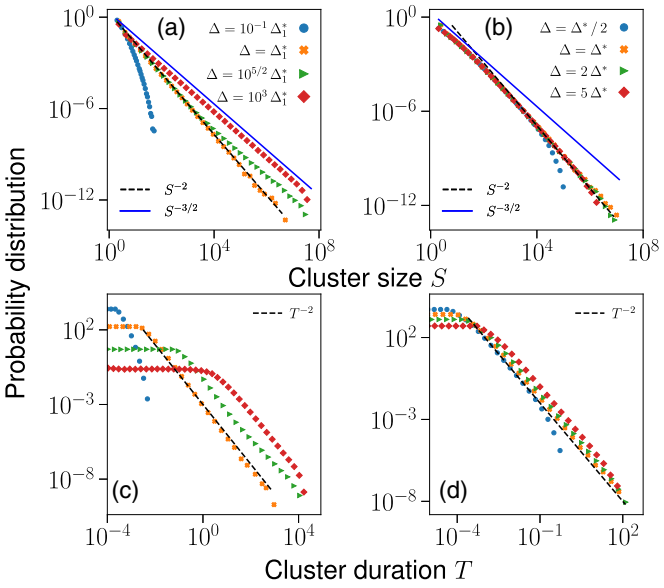

FIG. 2. Critical properties of self-exciting temporal processes. We consider processes generated from the rate of Eq. (1) with exponential kernel and $n = 1$. System size $K = 10^8$. Histograms obtained by considering $C = 10^7$ clusters per configuration. (a) Cluster size distribution for $\mu = 10^{-4}$. (b) Cluster size distribution for $\mu = 10^2$. (c) Cluster duration distribution for the same data as in panel (a). (d) Cluster duration distribution for the same data as in panel (b).

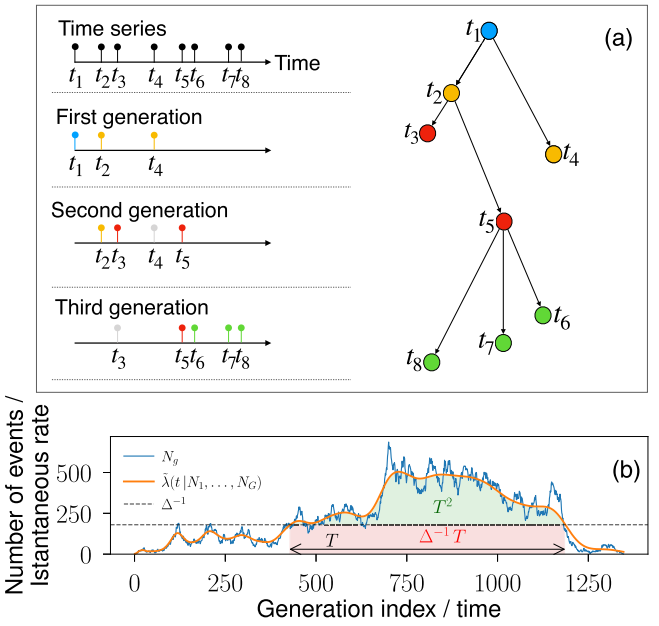

FIG. 3. Latent tree structure of self-exciting temporal processes. (a) Each event in the time series on the left is associated to a parent node. On the right, the branching tree corresponding to the time series. Each node is assigned to a generation, and each bond has associated an interevent time. If N_g is the number of nodes in the gth generation, the depicted tree has $\{N_1 = 1, N_2 = 2, N_3 = 2, N_4 = 3, \ldots\}$. (b) The mapping of panel a allows us to associate to the tree $\{N_1, \ldots, N_G\}$ (blue curve) an inhomogeneous Poisson process with instantaneous rate $\tilde{\lambda}(t|N_1, \ldots, N_G)$ (orange). Such a process generates time series statistically equivalent to those generated by an Hawkes process with latent tree structure $\{N_1, \ldots, N_G\}$. The inverse resolution parameter Δ^{-1} (dashed black line) is an effective threshold for the Poisson process $\tilde{\lambda}(t|N_1, \ldots, N_G)$. As a result, size, and duration of clusters are related by Eq. (2). The shaded areas denote the two terms appearing on the rhs of Eq. (2).

the distribution $P(S)$ displays a neat crossover between the regime $\tau = 2$ for small S and the regime $\tau = 3/2$ at large S [Fig. 2(a)].

For $\mu \gg 1$, the phase diagram displays a single transition [Fig. 1(c)], with features identical to those described for the case $\mu \ll 1$ around Δ_1^*: no crossover is present, and the critical exponents of the distributions $P(S)$ and $P(T)$ are $\tau = \alpha = 2$ [Figs. 2(b) and 2(d)]. The same exact behavior can be obtained by simply considering a nonhomogeneous Poisson process with rate linearly growing in time, i.e., $\lambda(t) \sim t$ (see Ref. [28], Sec. K).

The two different behaviors observed for $\mu \ll 1$ and $\mu \gg 1$ are interpreted in an unified framework as follows. For $\mu \ll 1$, the process is characterized by a sequence of self-exciting bursts due to the memory term of the rate of Eq. (1). Memory decays exponentially fast, with a typical timescale equal to 1. Each burst is started by a spontaneous event. Since spontaneous events are characterized by the timescale $1/\mu \gg 1$, consecutive bursts are well separated one from the other. Increasing Δ, the system exhibits first a transition "within bursts" at $\Delta = \Delta_1^*$, corresponding to the merger of events within the same burst, and then a transition "across bursts" at $\Delta = \Delta_2^*$, corresponding to the merger of consecutive bursts of activity. For $\mu \gg 1$, all events belong to a unique burst of self-excitation. The timescale of spontaneous activity is equal or smaller than the one due to self-excitation. Thus, although the memory decays exponentially fast, a new spontaneous event reexcites the process quickly enough to allow the burst to proceed its activity uninterrupted. The burst is truncated in the simulations due to the fixed size K of the time series. As Δ increases, all events of the single burst are merged into a single cluster. The transition is therefore of the same type as the one observed within bursts at $\Delta = \Delta_1^*$ in the case $\mu \ll 1$.

We can separately study the transitions within and across bursts. To this end, we simplify the actual process of Eq. (1) by setting $\mu = 0$ and assuming that the first event of the burst already happened. We then invoke the known mapping of the self-exciting process of Eq. (1) to a standard Galton-Walton branching process (BP) [27]. According to it, the first event of the time series represents the root of a branching tree (Fig. 3). Each event generates a number of follow-up events (offsprings) obeying a Poisson distribution with expected value equal to n, the parameter appearing in Eq. (1). Time is assigned as follows. The first event happens at an arbitrary time t_1, say for simplicity $t_1 = 0$. Then each of the following events has associated a time equal to the time of its parent plus a random variate x extracted from the kernel function $\phi(x)$ of Eq. (1). The mapping to the BP offers an alternative (on average statistically equivalent) way of generating time series for the self-exciting process of Eq. (1). We first generate a BP tree, and then associate a time to each event of the tree according to the rule described above. The time t associated to a generic event of the gth generation is distributed according to a

function $P(t|g)$. For the exponential kernel function, $P(t|g)$ is the sum of g exponentially distributed variables, i.e., the Erlang distribution with rate equal to 1, $P(t|g) = t^{g-1}\, e^{-t}/(g-1)!$.

The mapping of the self-exciting process to a BP allows us to fully understand the numerical findings of Figs. 1 and 2. For $n = 1$ the BP is critical. The distribution of the tree size is $P(Z) \sim Z^{-3/2}$ and the distribution of the tree depth is $P(D) \sim D^{-2}$. Individual bursts of activity, as seen for sufficiently high Δ values and $\mu \ll 1$, obey this statistics. Specifically, the size of each burst S is exactly the size Z of the tree. The average duration of the bursts $\langle T \rangle \sim D$, as expected for the sum of iid exponentially distributed random variates. For $\Delta \in [\Delta_1^*, \Delta_2^*]$, P_∞ of Fig. 1(b) follows the same statistics as the maximum value of a sample of variables extracted from the distribution $P(Z) \sim Z^{-3/2}$ divided by their sum, and the average value of the ratio plateaus at $1 - 1/e$ for sufficiently large sample sizes, fully explaining the results of Fig. 1 (see Ref. [28], Sec. H).

The behavior at $\Delta = \Delta_1^*$ and the crossover towards the standard BP regime for larger Δ are due to a threshold phenomenon. This directly follows from the abrupt nature of the percolation transition of the Poisson process [Fig. 1(a)]. Given the latent branching tree $\{N_1, N_2, \ldots, N_g, \ldots, N_G\}$, where N_g indicates the number of events of the gth generation of the tree, the time series of the Hawkes process is statistically equivalent to the one of the inhomogeneous Poisson process with instantaneous rate $\tilde{\lambda}(t|N_1, \ldots, N_G) = \sum_g P(t|g) N_g$. Hence, for a given Δ, as long as $\tilde{\lambda}(t|N_1, \ldots, N_G) > 1/\Delta$, all events are part of the same cluster of activity; when instead $\tilde{\lambda}(t|N_1, \ldots, N_G) < 1/\Delta$, then events around time t belong to separate clusters of activity. As a consequence, the total number of events S_T that form a cluster of activity of duration T is the integral of the curve $\tilde{\lambda}(t|N_1, \ldots, N_G)$ in the time interval when the rate is above Δ^{-1} [Fig. 3(b)]. We repeat a similar calculation as in Ref. [19]. The integral can be split in two contributions, one corresponding to the area of the order of T^2 appearing above the threshold line, as expected for a critical BP [19,36], and the other corresponding to the area $\Delta^{-1}\, T$ appearing below threshold,

$$S_T \sim T^2 + \Delta^{-1}\, T. \tag{2}$$

While the distribution of cluster durations is always the same [i.e., $P(T) \sim T^{-2}$ of the underlying BP], if $\Delta^{-1} > T$, then $S_T \sim T$ implying the within-burst statistics $P(S) \sim S^{-2}$. Instead, if $\Delta^{-1} < T$, then $S_T \sim T^2$ and the conservation of probability leads to the BP statistics $P(S) \sim S^{-3/2}$. When the two terms on the rhs of Eq. (2) have comparable magnitude, a crossover between the two scalings occurs. The crossover point varies with the temporal resolution as $S_c \propto \Delta^{-2}$ (see Ref. [28], Sec. G). A full understanding of $P(S)$ is achieved by noting that power-law scaling requires a minimum sample size to be observed, sufficient for the largest cluster to have duration comparable to $1/\Delta_1^*$. If the sample is not large enough, the distribution will appear as exponential (see Ref. [28], Sec. G).

We finally consider the power-law kernel function $\phi(x) = (\gamma - 1)(1 + x)^{-\gamma}$. The branching structure underlying the process is not affected by the kernel, so the results above should continue to hold [21]. For $\gamma > 2$, $\phi(x)$ has finite mean value, and, as a consequence, results are identical to those obtained for the exponential kernel (see Ref. [28], Sec. G). Specifically, P_∞ shows a discontinuous transition when $\mu \gg 1$, while two sharp transitions are observed for $\mu \ll 1$. The distribution of cluster sizes exhibits a crossover from $\tau = 2$ at Δ_1^* to $\tau = 3/2$ for $\Delta \gg \Delta_1^*$ when $\mu \ll 1$, and the exponent $\tau = 2$ with no crossover when $\mu \gg 1$. If $\gamma \leqslant 2$, $\phi(x)$ has a diverging mean value, and the typical interevent time is large preventing the present framework from being applicable.

In summary, we investigated how self-excitation mechanisms are reflected in the bursty dynamics, exploring their relationship with avalanche distributions, which offer an effective probe into the presence of autocorrelation in time series [1]. We focused on the Hawkes process, a general mechanism to produce self-excitation, autocorrelation, and fat-tailed distributions in the avalanche size and duration. Critical behavior in the distributions is observed at specific values of the resolution parameter Δ and is characterized by exponents independent of the form of the self-excitation mechanism. The universal critical behavior is governed by both the branching structure underlying the Hawkes process and the features of 1D percolation. Nontrivial details of the size distribution depend on the relative force of the spontaneous and self-excitation mechanisms. The two classes of behavior coexist for a wide range of Δ values, thus making the observation of a mixture of two classes the most likely outcome of an analysis where the resolution parameter is not fine-tuned. All findings extend to the slightly subcritical configuration of the Hawkes process (see Ref. [28], Sec. I), thus showing that our method is scientifically sound also for the analysis of avalanches in some natural systems possibly operating close to, but not exactly in, a critical regime [37]. Our work offers an interpretative framework for the relationship between avalanche properties and the mechanisms producing autocorrelation in bursty dynamics. More work in this area is nevertheless needed. The Hawkes process is unable to reproduce the variety of critical behaviors reported for real data sets in Ref. [1], and other self-excitation mechanisms need to be considered.

D.N. and F.R. acknowledge partial support from the National Science Foundation (Grant No. CMMI-1552487).

[1] M. Karsai, H.-H. Jo, and K. Kaski, *Bursty Human Dynamics* (Springer, 2018).
[2] L. Dalla Porta and M. Copelli, PLoS Comput. Biol. **15**, e1006924 (2019).
[3] J. M. Beggs and D. Plenz, J. Neurosci. **23**, 11167 (2003).
[4] P. Bak, K. Christensen, L. Danon, and T. Scanlon, Phys. Rev. Lett. **88**, 178501 (2002).
[5] F. Wang and Z. Dai, Nat. Phys. **9**, 465 (2013).

[6] A.-L. Barabasi, Nature (London) **435**, 207 (2005).
[7] M. Karsai, K. Kaski, A.-L. Barabási, and J. Kertész, Sci. Rep. **2**, 397 (2012).
[8] J. P. Gleeson, J. A. Ward, K. P. O'Sullivan, and W. T. Lee, Phys. Rev. Lett. **112**, 048701 (2014).
[9] A. J. Fontenele, N. A. P. de Vasconcelos, T. Feliciano, L. A. A. Aguiar, C. Soares-Cunha, B. Coimbra, L. Dalla Porta, S. Ribeiro, A. J. Rodrigues, N. Sousa *et al.*, Phys. Rev. Lett. **122**, 208101 (2019).
[10] L. Weng, A. Flammini, A. Vespignani, and F. Menczer, Sci. Rep. **2**, 335 (2012).
[11] H.-H. Jo, J. I. Perotti, K. Kaski, and J. Kertész, Phys. Rev. E **92**, 022814 (2015).
[12] P. Kumar, E. Korkolis, R. Benzi, D. Denisov, A. Niemeijer, P. Schall, F. Toschi, and J. Trampert, Sci. Rep. **10**, 626 (2020).
[13] V. Pasquale, P. Massobrio, L. Bologna, M. Chiappalone, and S. Martinoia, Neuroscience **153**, 1354 (2008).
[14] J. P. Neto, F. P. Spitzner, and V. Priesemann, arXiv:1910.09984.
[15] S. R. Miller, S. Yu, and D. Plenz, Sci. Rep. **9**, 16403 (2019).
[16] M. Chiappalone, A. Novellino, I. Vajda, A. Vato, S. Martinoia, and J. van Pelt, Neurocomputing **65**, 653 (2005).
[17] A. Levina and V. Priesemann, Nat. Commun. **8**, 15140 (2017).
[18] S. Janićević, L. Laurson, K. J. Måløy, S. Santucci, and M. J. Alava, Phys. Rev. Lett. **117**, 230601 (2016).
[19] P. Villegas, S. di Santo, R. Burioni, and M. A. Muñoz, Phys. Rev. E **100**, 012133 (2019).
[20] A. G. Hawkes, Biometrika **58**, 83 (1971).
[21] A. Helmstetter and D. Sornette, J. Geophys. Res.: Solid Earth **107**, ESE 10-1 (2002).
[22] Y. Ogata, J. Am. Stat. Assoc. **83**, 9 (1988).
[23] F. Y. Kalle Kossio, S. Goedeke, B. van den Akker, B. Ibarz, and R.-M. Memmesheimer, Phys. Rev. Lett. **121**, 058301 (2018).
[24] R. Crane and D. Sornette, Proc. Natl. Acad. Sci. USA **105**, 15649 (2008).
[25] D. Sornette, F. Deschâtres, T. Gilbert, and Y. Ageon, Phys. Rev. Lett. **93**, 228701 (2004).
[26] D. Stauffer and A. Aharony, *Introduction to Percolation Theory* (Taylor and Francis, London, 1994).
[27] A. G. Hawkes and D. Oakes, J. Appl. Probab. **11**, 493 (1974).
[28] See Supplemental Material at http://link.aps.org/supplemental/10.1103/PhysRevE.103.L020302 for a detailed description of the numerical simulations and of the analysis performed, additional results from numerical simulations, and a full development of the theory presented in this paper. The Supplemental Material includes Refs. [29–33].
[29] Y. Ogata, IEEE Trans. Inf. Theory **27**, 23 (1981).
[30] M.-A. Rizoiu, Y. Lee, S. Mishra, and L. Xie, arXiv:1708.06401.
[31] A. Dassios and H. Zhao, Adv. Appl. Probab. **43**, 814 (2011).
[32] P. Colomer-de Simón and M. Boguñá, Phys. Rev. X **4**, 041020 (2014).
[33] M. Boguná, R. Pastor-Satorras, and A. Vespignani, Eur. Phys. J. B **38**, 205 (2004).
[34] D. Stauffer and C. Jayaprakash, Phys. Lett. A **64**, 433 (1978).
[35] A. Dassios and H. Zhao, Electron. Commun. Probab. **18**, 1 (2013).
[36] S. di Santo, P. Villegas, R. Burioni, and M. A. Muñoz, Phys. Rev. E **95**, 032115 (2017).
[37] V. Priesemann, M. Wibral, M. Valderrama, R. Pröpper, M. Le Van Quyen, T. Geisel, J. Triesch, D. Nikolić, and M. H. Munk, Front. Syst. Neurosci. **8**, 108 (2014).